J Solid State Electrochem (2011) 15:675–681
DOI 10.1007/s10008-010-1131-8

ORIGINAL PAPER

The preparation and performance of flocculent polyaniline/carbon nanotubes composite electrode material for supercapacitors

Liping Zheng · Xianyou Wang · Hongfang An · Xingyan Wang · Lanhuan Yi · Li Bai

Received: 7 February 2010 / Revised: 21 April 2010 / Accepted: 17 June 2010 / Published online: 8 July 2010

Abstract Polyaniline (PANI)/carbon nanotubes (CNTs) composite electrode material was prepared by in situ chemical polymerization. The structure and morphology of PANI/CNTs composite are characterized by Fourier infrared spectroscopy, scanning electron microscope, and transmission electron microscopy. It has been found that a flocculent PANI was uniformly deposited on the surface of CNTs. The supercapacitive behaviors of the PANI/CNTs composite materials are investigated with cyclic voltammetry, galvanostatic charge/discharge, impedance, and cycle life measurements. The results show that the PANI/CNTs composite electrodes have higher specific capacitances than CNT electrodes and better stability than the conducting polymers. The capacitance of PANI/CNTs composite electrode is as high as 837.6 F g^{-1} measured by cyclic voltammetry at 1 mV s^{-1}. Besides, the capacitance retention of coin supercapacitors remained 68.0% after 3,000 cycles.

Keywords Carbon nanotubes · Polyaniline · Composite electrode · Electrochemical performance · Supercapacitor

Introduction

Supercapacitors have attracted great interest because they combine the advantages of the high specific power of dielectric capacitors and the high specific energy of rechargeable batteries [1]. The energy storage of supercapacitors based on double layer is the accumulation of ionic charges which occur at the electrode/electrolyte interface. So the high specific surface area (SSA) and the porosity of carbon electrode materials are the basic requirements to achieve high specific capacitance. Carbon nanotubes (CNTs) are frequently studied for supercapacitor applications since their discovery [2] because of their unique mesoporous network with high accessible surface area, excellent electrical conductivity, and chemical stability [3]. However, the CNTs only possess lower double-layer capacitance, while metal oxides and electronically conducting polymer (ECP) possess huge Faradaic capacitance, and the Faradaic pseudocapacitance is almost 10~100 times higher than double-layer capacitance [4]. In order to improve the supercapacitive performances of CNT electrode, various metal oxides/CNTs and ECP/CNTs composites have been synthesized recently [5, 6]. Among these materials, polyaniline (PANI) has been considered as one of the most promising polymer material in supercapacitors due to its oxidation–reduction properties, high SSA, environmental stability [7, 8] as well as relatively easy polymerization in aqueous media. Therefore, an improvement in the capacitance of CNTs can be obtained by preparing PANI/CNTs composites.

Over the years, much attention has been paid to the synthesis of PANI/CNT composite materials with highly electrochemical performances by controlling the different morphologies of PANI, including nanotubes [9], hollow PANI microspheres [10], and whisker-like PANI [11], which have been obtained by changing the synthesis methods. Meng et al. [12] reported a novel chemical oxidative polymerization of polyaniline/multiwalled carbon nanotubes (PANI/MWCNT) paper-like composites, with the highest specific capacitances of 424 F g^{-1} obtained at 200 mA g^{-1}, and it lost 10.6% of its initial

L. Zheng · X. Wang (✉) · H. An · X. Wang · L. Yi · L. Bai
School of Chemistry, Key Laboratory of Environmentally Friendly Chemistry and Applications of Minister of Education, Xiangtan University,
Hunan 411105, China
e-mail: wxianyou@yahoo.com

specific capacitance after 1,000 cycles. Zhang et al. [13] synthesized PANI/MWCNT composite films by in situ electrochemical polymerization and obtained the highest specific capacitance value of 500 F g^{-1} for the PANI/MWCNT composite film containing only 0.8 wt.% MWCNT, while the specific capacitance of the PANI/MWCNT composites decreased about 32% after 1,000 charge/discharge cycles. Based on the potential superiority of CNTs and PANI, there are still many researchers studying on PANI/CNTs composite in order to seek preferable morphologies and high electrochemical performances for the applications of supercapacitors.

Recently, our group has successfully synthesized the calcium carbide-derived carbon/polyaniline (CCDC/PANI) [14] and polyaniline/carbon aerogel (PANI/CA) [15] composite electrode materials by chemical oxidation polymerization and obtained the high specific capacitances of 713.4 and 710.7 F g^{-1}, respectively. In this work, we prepared a flocculent PANI/CNTs composite by adsorption of aniline on the surface, followed by in situ chemical polymerization, and used as the electrode material of supercapacitors. The results revealed that the PANI/CNTs composite electrodes show much higher specific capacitance, better cyclic stability, and more promise for applications in supercapacitors than that was reported before. The structure characterization and electrochemical performance measurements of PANI/CNTs composite were discussed in detail.

Experimental section

Material synthesis

The pre-treatment of CNTs

The multiwalled CNTs were obtained from Chengdu Institute of organic chemistry (the purity of the pristine CNTs was 99% and 20–30-nm diameter). CNTs were treated by ball-milling method and then treated with 2 mol L^{-1} HNO_3 solution, shaken for 6 h at 70 °C, then filtrated and washed with distilled water till the pH value of the filtrate reached 7. The resultant-activated CNTs were dried in vacuum at 80 °C for 24 h.

The synthesis of PANI/CNTs composite

The PANI/CNTs composite was prepared by adsorption of aniline followed by in situ chemical polymerization with ammonium peroxodisulfate, and its synthesis route of PANI/CNTs composite is schematically represented in Fig. 1. The detailed preparation process can be described as follows: (1) Activated CNTs (0.5 g) were immersed in ethanol solution (100 mL, 20%, containing 1.4 g aniline and 10 g H_2SO_4) while being stirred under vacuum for 1 h; (2) ethanol solution (100 mL, 20 %) was added to the above-mentioned solution quickly with intensive stirring; (3) ammonium persulfate solution (the mass ratio of aniline/ammonium persulfate is 1:2.3) was added drop by drop to the solution mentioned in step 2 which was stirred at 0 °C for 5 h. The black–green product of the reaction was filtered and washed repeatedly with distilled water and alcohol. The resulting composite was dried under vacuum at 50 °C for 24 h. The 70 wt.% mass load of PANI in the composite was determined by calculating the weight difference of CNTs.

Measurements of physical and chemical properties

1. The Fourier infrared spectroscopy (FTIR) measurements of different samples were performed with a FTIR spectrometer (Perkin-Elmer Spectrum one) in the wave number range from 4,000 to 500 cm^{-1}, using the KBr disk method.
2. The morphology of the PANI/CNTs composite was observed using a scanning electron microscope (JSM-6700F).
3. The transmission electron microscopy (TEM) of the PANI/CNTs composite was performed using a FEI Tecnai G2 microscope at 200 kV.

Preparation of the PANI/CNT composite electrodes and electrochemical measurements

The mixture containing 80 wt.% PANI/CNT composites, 10 wt.% carbon black, and 10 wt.% polytetrafluoroethylene was well mixed and then pressed onto a stainless steel grid (1.6×10^7 Pa) that served as a current collector (geometric area was 1.5 cm^2). The mass load of the as-prepared electrode was 5 mg cm^{-2}. The electrochemical performances of the electrodes were characterized by cyclic voltammetry (CV) and impedance spectroscopy test. The used electrolyte was 1 M H_2SO_4 solution. The experiments were carried out using a three-electrode system, in which steel and the saturated calomel electrodes (SCE, 0.242 V vs. the normal hydrogen electrode) are used as counter and reference electrodes, respectively. The charge/discharge and the cycle life measurements at constant current were carried out by potentiostat/galvanostat on button cell supercapacitors.

Results and discussion

Material characterization

FTIR spectra of CNTs and PANI/CNTs composite are shown in Fig. 2. Characteristic peaks at 3,414 and

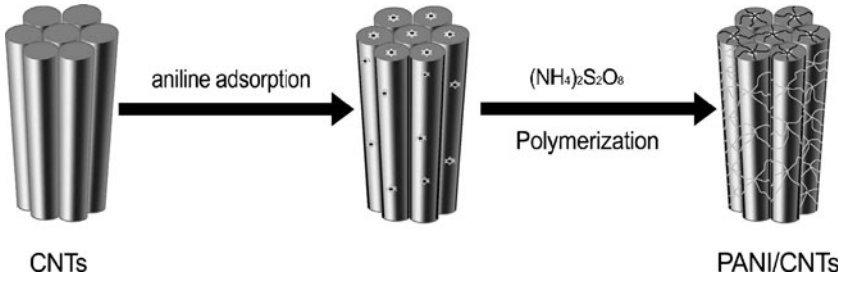

Fig. 1 Schematic preparing process of PANI on the surface of CNTs

1,160 cm^{-1} are observed in the FTIR spectrum of the initial CNTs material. These peaks can be ascribed to –OH (3,500 cm^{-1}) and C–C–O (1,096 cm^{-1}) stretching vibration band, respectively. About in the 1,600 cm^{-1}, two faint characteristic peaks can be seen, which present the stretching vibration peaks of oxygenous functional groups after HNO_3 treatment. As to PANI/CNTs composites, the 1,558-cm^{-1} band was characteristics of the nitrogen quinone (Q) structure, and 1,478 cm^{-1} was related to the benzenoid structure (B). The bands in the range 1,200–1,400 cm^{-1} are the C–N stretching band of an aromatic amine, such as 1,301 (QBQ) and 1,244 cm^{-1} (QBQ, QBB, BBQ) [11]. A strong band characteristically appears at 1,108 cm^{-1}, which has been explained as an electronic band or vibration band of nitrogen quinone (N=Q=N). The C–H out of plane bending mode has been used as a key to identify the type of substituted benzene. This mode was observed in PANI as a single band at 801 cm^{-1}. This meant that PANI was 1,4 substituted [16], and the possible chemical structure of PANI was shown in Fig. 2. Comparing two FTIR spectra, it can be found that PANI exists apparently on the surface of CNTs.

The morphologies and microstructures of the CNTs and PANI/CNTs composite have been examined by scanning electron microscopy (SEM) and transmission electron microscopy (TEM). Figure 3 shows SEM and TEM images of CNTs and PANI/CNTs composite. As being seen from Fig. 3a, c, the surface of activated CNTs became rough after being treated with HNO_3, and some of them were broken into several parts by ball-milling method, which can increase the surface area and the dispersion or wetting of CNTs in aniline monomer. For the CNTs coated PANI (Fig. 3b), a layer of flocculent deposit coated homogenously the surface of CNTs, which was attributed to the freshly deposited PANI. As shown in the TEM image of the PANI/CNTs composite (Fig. 3d), it can be seen that a clear morphology change takes place on the external surface of the CNTs due to surface modification of PANI. Nevertheless, it still keeps the advantage of the entangled network of the nanotubes that allows a good access of the electrolyte to the active polymer material. There is no doubt that such texture of the capacitor electrodes is optimal for the fast ion diffusion and migration in the polymer which can increase more active sites of the composite for Faradaic reaction [17].

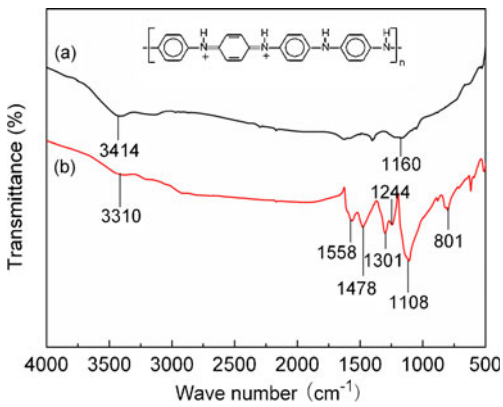

Fig. 2 FTIR spectra of **a** CNTs and **b** PANI/CNTs composite

Electrochemical characterization

In order to evaluate the electrochemical characteristics of PANI/CNTs composite, CV, and galvanostatic charge/discharge were used to characterize the electrochemical capacitive performance. Figure 4a shows cyclic voltammograms (within the potential window from −0.2 to 0.8 V vs. SCE) at different scan rates for the PANI/CNT electrodes. It can be found that the capacitance characteristic of the PANI phase is different from that of the electric double-layer capacitance (CNTs), which would produce a *C–V* curve close to the ideal rectangular shape. Two redox peaks in Fig. 4 are attributed to the redox transition of PANI between a semi-conducting state (leucoemeraldine form) and a conducting state (polaronic emeraldine form) and the emeraldine–pernigraniline transformation [18]. The two couples of redox peaks (C_1/A_1 and C_2/A_2) observed in Fig 4a result in the redox capacitance. With the increasing of scanning rate, the redox current of PANI/CNTs electrode increases clearly, indicating its good rate ability. The maximum specific capacitance of PANI/CNTs electrode was 837.6 F g^{-1} at 1 mV s^{-1} from the *C–V* curve according to the Eq. 1 [14]. This value is apparently higher than

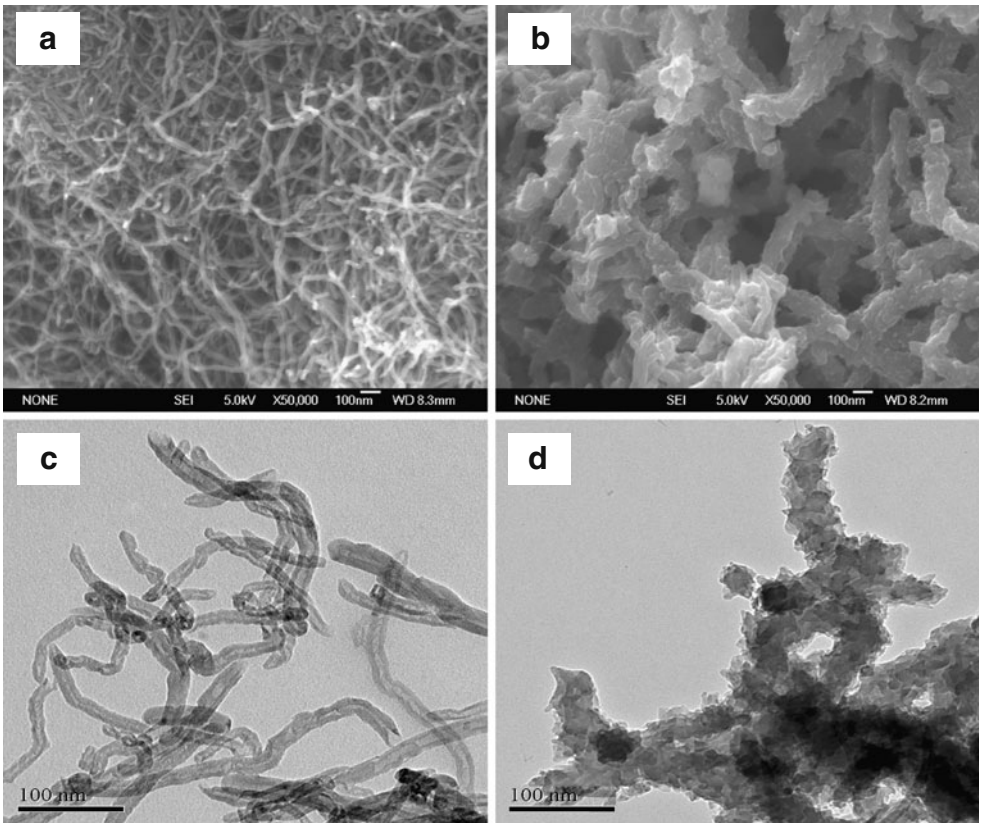

Fig. 3 SEM and TEM images of CNTs and PANI/CNTs composites. **a** SEM image of CNTs, **b** SEM image of PANI/CNTs, **c** TEM image of CNTs, **d** TEM image of PANI/CNTs

PANI/MWCNT composites reported by Meng et al. [12] and Zhang et al. [13].

$$C \equiv \frac{Q}{V} = \int \frac{i\mathrm{d}t}{\Delta V} \tag{1}$$

where i is a sampled current, dt is a sampling time span, and ΔV is a total potential deviation of the voltage window.

Cyclic voltammograms for the CNTs electrode and PANI/CNTs composite electrodes at 1 mV s^{-1} are shown in Fig. 4b. Comparing the CV of CNTs, it can be found that PANI/CNTs composite electrode has two couples of redox peaks, and the area surrounded by C–V curve is apparently larger than one of the CNTs electrode, indicating that the PANI/CNTs electrode has huge pseudocapacitance. Figure 5 illustrates schematic mechanism of pseudocapacitance of conducting polymer. The deposited PANI is uniformly coated around the CNTs. When the PANI is being charged, it loses electrons and becomes polycations, causing the anions in the solution to intercalate into the PANI in order to maintain electro-neutrality [4, 15]. The flocculent PANI creates electrochemical accessibility for electrolyte ions and reduces the distance within the PANI bulk where ions must be transported during the charging or discharging process. It is fundamental for electrode materials of supercapacitors to show high specific capacitance and high-rate charge/discharge ability.

Table 1 tabulates the specific capacitances of CNTs and PANI/CNTs composite at different potential sweep rates, which were calculated according to Eq. 1 based on C–V measurements. It can be found from Table 1 that the specific capacitances of PANI/CNTs electrodes are obviously higher than that of CNTs at every given scanning rate. Although coating PANI on CNTs will decrease the specific surface area of PANI/CNTs electrode and result in the decrease of the double-layer capacitance, PANI on PANI/CNTs electrode can produce a very big pseudocapacitance. The resulted pseudocapacitance is so big that the PANI/CNTs electrode has still a big specific capacitance except for making up the loss of double-layer capacitance.

The charge/discharge curves of PANI/CNTs electrodes measured at different current densities within a potential window (−0.2 to 0.8 V vs. SCE) are showed in Fig. 6a. As shown in Fig. 6a, discharge time increased distinctly with the decrease of current density, and the P–t relationships on these chronopotentiograms are approximately linear, indicating that the PANI/CNTs electrodes behave as capacitors and have a good cycling stability [15].

In Fig. 6b, the comparison of galvanostatic charge/discharge curves for the CNTs electrode and PANI/CNTs composite electrode at 500 mA g^{-1} was given. Comparing

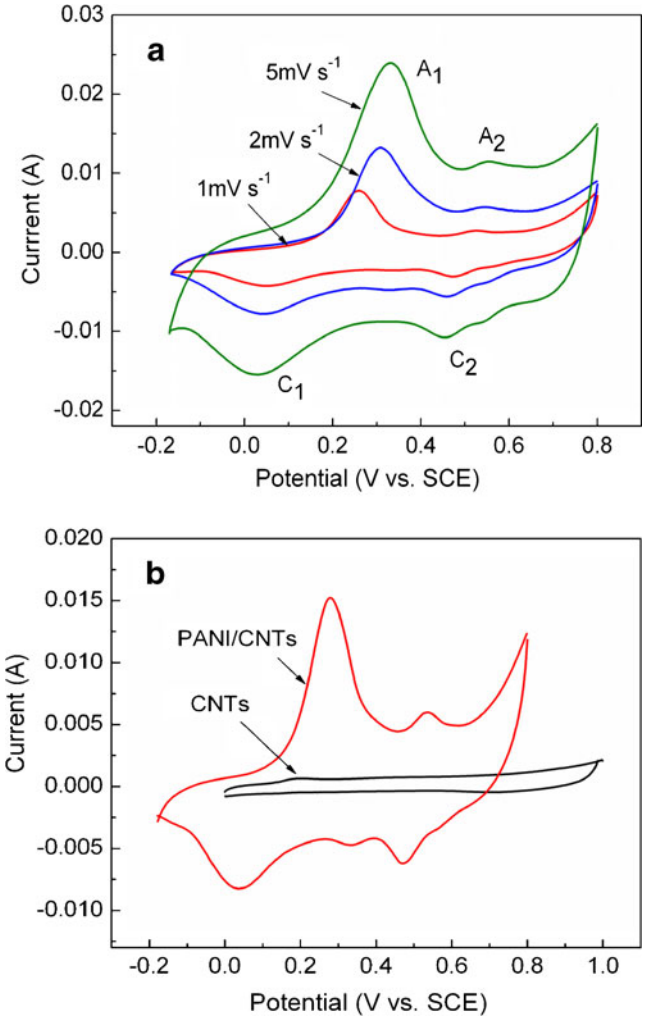

Fig. 4 Cyclic voltammograms for **a** PANI/CNTs electrodes at different scan rates and **b** the comparison of CNTs and PANI/CNTs composite at 1 mV s^{-1}

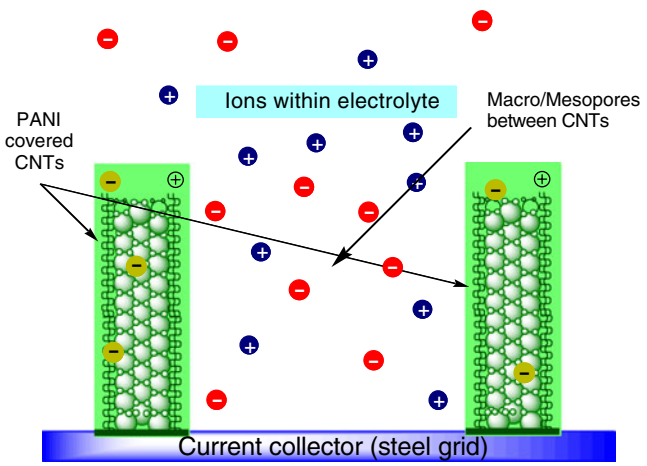

Fig. 5 Illustration of pseudocapacitance process in PANI/CNTs composites

Table 1 The specific capacitances of CNTs and PANI/CNTs composites

	Specific capacitance of supercapacitors (Fg^{-1})			
	$1mVs^{-1}$	$2mVs^{-1}$	$5mVs^{-1}$	$10mVs^{-1}$
CNTs	64.5	58.3	55.6	49.6
PANI/CNTs	837.6	765.0	646.4	538.6

with the charge/discharge curve of CNTs, in which the potential varies nearly linearly with time, while curves of PANI/CNTs electrodes deviate from ideal linear line, indicating that the specific capacitance of the composite electrode is composed of both the double-layer capacitance of CNTs and Faradaic capacitance of PANI.

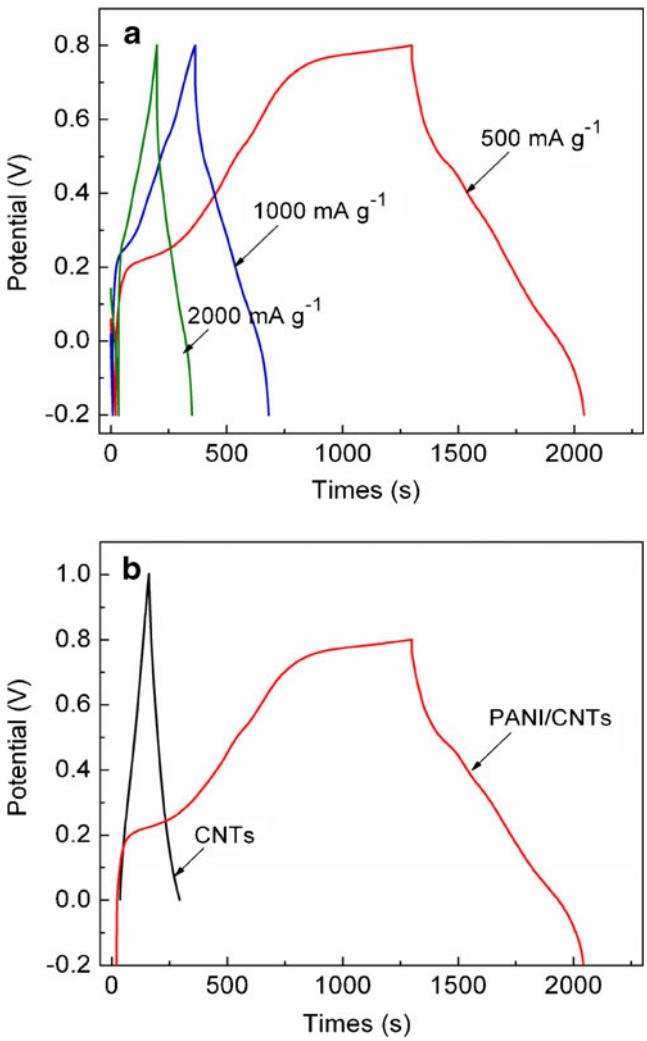

Fig. 6 Charge/discharge curves for **a** PANI/CNTs electrode at different current density and **b** comparison of CNTs and PANI/CNTs composites at 500 mA g^{-1}

The electrochemical impedance spectroscopy (EIS) (100 kHz–10 mHz) of CNT and PANI/CNT composite electrodes are shown in Fig. 7. The principal objective of the EIS experiments is to gain the interfacial properties (capacitance, electron-transfer resistance) of electrodes. The semicircle portion observed at higher frequencies corresponds to the electron-transfer-limited process, whereas the linear part is characteristic of the lower frequencies range and represents the diffusion-limited electrode process. In order to obtain more information from the EIS results, we model the working electrode using an equivalent circuit (insert in Fig. 7). As shown in the equivalent circuit, it can be seen that double-layer capacitance C_{dl} is in parallel with a Faradaic resistance R_F, and then the mentioned part is in series with the uncompensated electrical resistance R_Ω and the Faradaic pseudocapacitance C_F of PAN-based film [19]. Moreover, R_Ω is the summation of the electrode of active materials (R_a), the electrolyte (R_e), and the electrical leads combined (R_1). The introduction of PANI into PANI/CNTs composites increase the R_a and thus increase the R_Ω.

From the comparison of two semicircles in the high frequency region, it also shows that the charge-transfer complex resistance of the PANI/CNTs composite (2.348 Ω) is slightly larger than that of the pure CNTs (0.216 Ω); the reason is probably attributable to the relative poor movement of the electrolyte ions in polymer [15], which is the most important factor influencing the cycle stability of composite.

In order to gain a further understanding on the electrochemical performances of PANI/CNTs composite materials, CNTs and PANI/CNTs were used as electrode active materials of symmetrical coin supercapacitors, respectively. The dependences of the specific capacitance of the two coin supercapacitors with charge/discharge cycle number are shown in Fig. 8. It is found that the CNTs and PANI/CNTs supercapacitors have demonstrated a very long cycle life under shallow depths of discharge. The specific capacitance of the coin supercapacitors can be known from Eq. 2 [20].

$$C = \frac{2Q}{mV} = 2 \times 3,600 \times 0.001 \times \frac{C^*}{mV} = 7.2 \times \frac{C^*}{mV} \qquad (2)$$

where C is the specific capacitance of the supercapacitor, in Farad per grams; Q is electric quantity, coloumbs; C^* is the capacitance measured, milliampere hour; m is the weight of simple electrode, grams; and V is the range of the charge/discharge, volts.

The capacitance retentions of the two coin supercapacitors over 3,000 cycles are 99.5% and 68.0% for CNTs and PANI/CNTs, respectively. The big capacitance loss of PANI/CNTs supercapacitor during cyclic process is probably because larger PANI loading results in the existence of larger scale of PANI phase and will cause crack during charge/discharge process. In addition, the part of the PANI deposits loses contact with the CNTs and results in not only poor transport of electrons but also poor ion movement [15, 21]. Even so, the specific capacitance of PANI/CNTs supercapacitor is clearly higher than that of CNTs supercapacitor; furthermore, although the capacitance loss of PANI/CNTs supercapacitor (Fig. 8) is obviously larger than that of CNTs, the specific capacitance of PANI/CNTs is still markedly higher than CNTs even after 3,000 charge/discharge cycles, which indicates that the PANI/CNTs will be a promising electrode active material for long-term supercapacitor applications. Of course, future work should focus on the improvement of cyclic stability of the PANI/CNTs composites and thus increase its cyclic life.

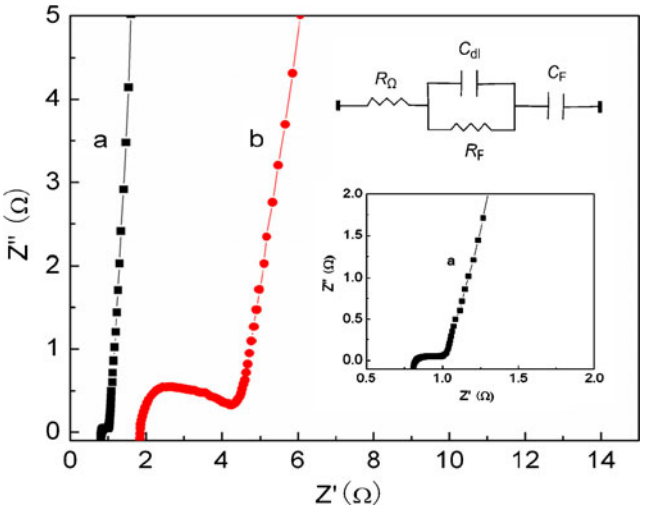

Fig. 7 Nyquist plots of **a** CNTs and **b** PANI/CNTs electrodes

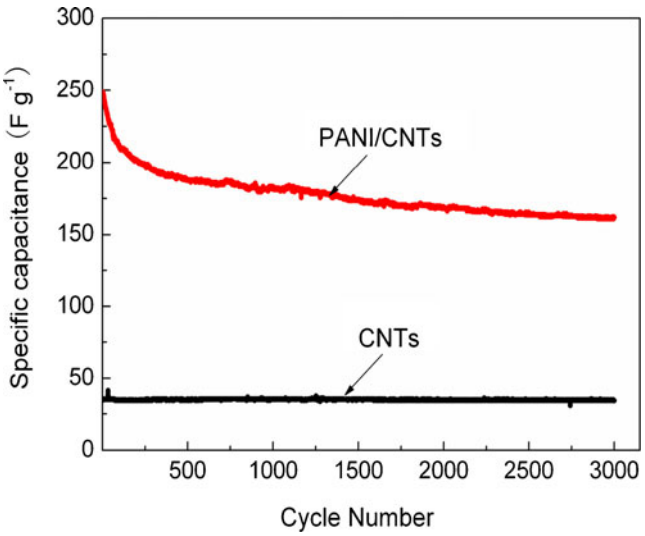

Fig. 8 Cycle life of CNTs and PANI/CNTs supercapacitors at 500 mA g^{-1} within the potential window −0.2 to 0.8 V

Conclusion

Flocculent PANI/CNT composite was prepared by in situ chemical oxidation polymerization of aniline adsorbed on CNTs. The capacitance of the PANI/CNTs supercapacitor is markedly higher than one of CNTs supercapacitor since the capacitance of the PANI/CNTs is the combination of double-layer capacitance (CNTs) and Faradaic pseudocapacitance (PANI). PANI/CNT composites in the application of supercapacitor showed obvious improvement in electrochemical performances, such as high specific capacitance, stable cycle life, and high-rate charge/discharge ability. The specific capacitance of PANI/CNTs electrode calculated from *C–V* curve is as high as 837.6 F g^{-1} at 1 mV s^{-1} compared with 64.5 F g^{-1} of CNT electrode. Besides the capacitance, retention of the coin supercapacitor using PANI/CNT composite as electrode active material was up to 68.0% after 3,000 cycles. Therefore, it is obviously proved that the PANI/CNTs composite is a promising electrode material for the applications of supercapacitors.

Acknowledgments This work was financially supported by the National Natural Science Foundation of China (grant no. 20871101) and Key Project of Education Department of Hunan Province Government (grant no. 2009WK2007).

References

1. Winter M, Brodd RJ (2004) Chem Rev 104:4245
2. Ijima S (1991) Nature 354:56
3. Gooding JJ (2005) Electrochim Acta 50:3049
4. Peng C, Zhang SW, Jewell D, Chen GZ (2008) Prog Nat Sci 18:777
5. Gao B, Yuan CZ, Su LH, Chen L, Zhang XG (2009) J Solid State Electrochem 13:1251
6. Kong LB, Zhang J, An JJ, Luo YC, Kang L (2008) J Mater Sci 43:3664
7. Cho SI, Lee SB (2008) Acc Chem Res 41:699
8. Lin YR, Teng H (2003) Carbon 41:2865
9. Gupta V, Miura N (2005) Electrochem Commun 7:995
10. Wei ZX, Wan MX (2002) Adv Mater 14:1314
11. Wang YG, Li HQ, Xia YY (2006) Adv Mater 18:2619
12. Meng CZ, Liu CH, Fan SH (2009) Electrochem Commun 11:186
13. Zhang J, Kong LB, Wang B, Luo YC, Kang L (2009) Synth Met 159:260
14. Zheng LP, Wang Y, Wang XY, Li N, An HF, Chen HJ, Guo J (2010) J Power Sources 195:1747
15. An HF, Wang Y, Wang XY, Li N, Zheng LP (2010) J Solid State Electrochem 14:651
16. Subramania A, Devi SL (2008) Polym Adv Technol 19:725
17. Zhang H, Cao GP, Wang WK, Yuan K, Xu B, Zhang WF, Cheng J, Yang YS (2009) Electrochim Acta 54:1153
18. Hu CC, Lin JY (2002) Electrochim Acta 47:4055
19. Zhou YK, He BL, Zhou WJ, Li HL (2004) J Electrochem Soc 151:A1052
20. Huang QH, Wang XY, Li J, Dai CL, Gamboa S, Sebastian PJ (2007) J Power Sources 164:425
21. Li LX, Song HH, Zhang QC, Yao JY, Chen XH (2009) J Power Sources 187:268